Astron. Astrophys. 245, L13–L16 (1991)

ASTRONOMY AND ASTROPHYSICS

Letter to the Editor

CO $J=1-0$, 2–1 and 3–2 absorption and emission toward the nucleus of Centaurus A*: probing the circumnuclear disk

F. P. Israel[1], E. F. van Dishoeck[1], F. Baas[1,2], T. de Graauw[3], and T. G. Phillips[4]

[1] Sterrewacht Leiden, P.O. Box 9513, NL-2300 RA Leiden, The Netherlands
[2] Joint Astronomy Centre, 665 Komohana Street, Hilo, HI 96720, USA
[3] Laboratory for Space Research, University of Groningen, P.O. Box 800, NL-9700 AV Groningen, The Netherlands
[4] Div. of Physics, Mathematics and Astronomy, California Institute of Technology 320–47, Pasadena CA 91125, USA

Received January 3, accepted March 19, 1991

Summary. High signal to noise spectra of ^{12}CO, ^{13}CO and $C^{18}O$ $J=1-0$, ^{12}CO 2–1 and ^{12}CO 3–2 have been obtained toward the nucleus of Centaurus A. The ^{12}CO profiles reveal the presence of two superposed emission components. The narrower component ($\Delta V \approx 70$–100 km s^{-1}) is due to CO emission from the dust lane. The broader component ($\Delta V \approx 260$ km s^{-1}) represents CO emission from the circumnuclear disk, whose presence was previously deduced from absorption line and infrared continuum observations. Analysis of the CO data suggests excitation temperatures of about 25 K in the circumnuclear disk. In both HCO^+ and CO spectra, weak absorption features are seen at red-shifted velocities, which probably represent warm and dense gas falling into the nucleus.

Key words: extragalactic: Centaurus A – NGC 5128; molecules: CO – HCO^+; galaxies: nuclei – circumnuclear disk

1. Introduction

NGC 5128 (Centaurus A) is not only one of the more interesting galaxies kinematically (Quillen et al. 1991), but it is also unique in having a strong nuclear millimetre continuum against which atomic and molecular lines are seen in absorption. Measurements at centimetre wavelengths have revealed absorption features due to OH and H_2CO (Gardner and Whiteoak 1976*a*, *b*), H I (van der Hulst, Golisch and Haschick 1983), C_3H_2 (Seaquist and Bell 1986; Bell and Seaquist 1988) and NH_3 (Seaquist and Bell 1990). In a recent paper (Israel et al. 1990; hereafter paper I), we presented spectra of the 2.6 millimetre CO $J=1-0$ line toward the nucleus, which show several narrow and deep absorption features superposed on a strong and broad emission line. These features are also seen in CO 2–1 spectra (Phillips, Sanders and Sargent 1990). In Paper I, we have argued that the absorption lines arise mostly in a circumnuclear disk of about 400 pc diameter. In order to study the physical properties of the absorbing material, we have started a program to measure a large number of molecular transitions in the millimetre and submillimetre range. Here we present high signal to noise spectra of the $J=1-0$ and 2–1 CO isotopes, as well as the first detection of strong CO 3–2 absorption and emission and some initial results from our search for other molecules. An independent study of absorption lines in Centaurus A has been carried out by Eckart et al. (1990), which focusses mostly on the strongest components seen in CO 1–0 and 2–1.

2. Observations

The observations up to 230 GHz were collected in several observing runs between January 1989 and July 1990 with the 15 m Swedish–ESO Submillimetre Telescope (SEST) at La Silla, Chile. At frequencies up to 115 GHz (^{12}CO 1–0), the Schottky barrier diode receiver provided single side band (SSB) system temperatures including sky of about 500 K. At higher frequencies around 230 GHz (^{12}CO 2–1), the SSB system temperature was about 1000 K. For the back-end, we used primarily the high-resolution acousto-optical spectrometer (AOS) consisting of 2048 channels with a width of 50 kHz, resulting in velocity resolutions of about 0.13 km s^{-1} and 0.06 km s^{-1} at 115 and 230 GHz, respectively. Whenever possible, the low resolution backend (bandwidth 500 MHz, resolution 1 MHz) was used in parallel to obtain information on the emission profile and baseline. Total on-source integration times, summed over the various observing runs, were of order 1–4 hours. The main beam efficiencies are 0.71 and 0.51 at 115 and 230 GHz, respectively.

The ^{12}CO 3–2 spectra were obtained in March 1990 at the Caltech Submillimeter Observatory[1] (CSO) with the 345 GHz SIS receiver (Ellison et al. 1989). The spectra were taken under

Send offprint requests to: F. P. Israel

* Based in part on observations collected at the Swedish-ESO Submillimetre Telescope at the European Southern Observatory (ESO), La Silla, Chile

[1] The CSO is operated by the California Institute of Technology under funding from the National Science Foundation, Contract #AST-88-15132

excellent conditions, resulting in total system temperatures of 800–1000 K. The main beam efficiency is 0.60. A spectrum with a total on-source integration time of 2 hours was obtained with the wide band AOS, which has an effective velocity resolution of about 0.9 km s^{-1} at 345 GHz. A shorter integration (about 1 hour) was obtained with the high-resolution (0.04 km s^{-1}) AOS. The CSO beam size at 345 GHz is about 20″ FWHM, comparable to the SEST beam size at 230 GHz, but much smaller than the SEST beam at 115 GHz of 44″.

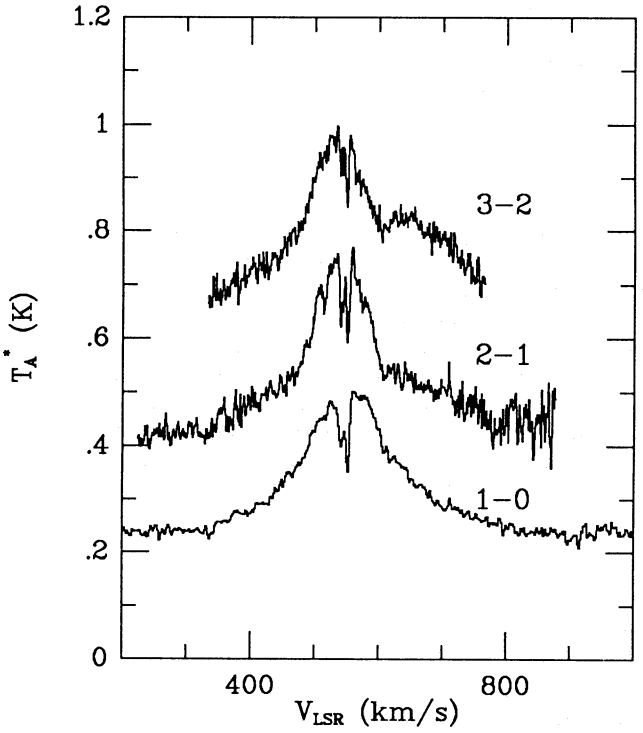

Fig. 1. ^{12}CO 1–0, 2–1 and 3–2 spectra toward the nucleus of Centaurus A, smoothed to 2.8, 0.9 and 0.9 km s^{-1} resolution. The 2–1 and 3–2 spectra have been shifted in T_A^* by +0.25 and +0.45 K respectively.

3. CO emission from the circumnuclear disk

In Figure 1, we present the observed ^{12}CO J=1–0, 2–1 and 3–2 profiles. The latter two clearly show a broad plateau (ΔV=260±10 km s^{-1}) underlying narrower emission (ΔV=70±7 km s^{-1}). The broad plateau is also present in the J=1–0 profile, but is less obvious there because of the greater width of the narrow profile ($\Delta V \approx$115 km s^{-1}). The narrow profile is due to extended emission from the dust lane. Its observed width reflects the overall rotation of the galaxy: it grows less with decreasing beam size ($\Delta V \approx$ 115 km s^{-1} in a 44″ beam (J=1–0 SEST); $\Delta V \approx$105 km s^{-1} in a 32″ beam (J=2–1 CSO: Phillips et al. 1987) and $\Delta V \approx$70 km s^{-1} in a 21″ beam (J=2–1 SEST; J=3–2 CSO)). In the 2–1 ^{12}CO SEST profile, the broad plateau is centered on V_{LSR}=554±5 km s^{-1}, which is within the error of the systemic velocity.[2]

[2] Throughout this paper we use $V_{LSR}=V_{Hel}$+2.1 km s^{-1}.

In the 3–2 CSO profile, its central velocity is about 570 km s^{-1}, but this is largely caused by a pronounced asymmetry on the red side. As the J=3–2 profile lacks extensive baseline coverage, the reality of this asymmetry is uncertain. A similar, but marginal asymmetry is seen in the 2–1 SEST profile. If real, it may indicate the presence of relatively hot material at red-shifted velocities, as has been found in M 82 in the J=6–5 transition (Stutzki 1990).

The plateau has T_{mb}(1–0)=160±30 mK, T_{mb}(2–1)=237±10 mK and T_{mb}(3–2)=223±15 mK, as determined from gaussian fits. Comparison of 1–0 and 2–1 observations with different beam sizes suggests that the plateau has a mean diameter of 34±4″, corresponding to 820 pc at the adopted distance of 5 Mpc. Thus, it must correspond to the circumnuclear disk inferred in Paper I from other observations, albeit with a radius somewhat larger than we estimated there. The velocity width of the plateau feature implies a total mass contained within the circumnuclear disk of $0.8 \times 10^9 < M_T < 6.3 \times 10^9$ $M_\odot$, if circular rotation is assumed with limits at R=50 and 400 pc. The gas-to-total mass ratio is $M_{gas}/M_T \approx$0.01 (cf. Paper I).

The observed brightness temperatures indicate a *mean* excitation temperature for all the circumnuclear gas in a 20″ beam of T_{ex}=25(+30, -10) K; locally, excitation temperatures may be higher than average. Because of the uncertainties in the true emission profile and in the decomposition, the excitation temperature of the narrow component corresponding to the dust lane is more difficult to determine, but is consistent with T_{ex}=10 K.

4. Absorption line forest

4.1. HCO^+ absorption: definition of the components

The various absorption components are most easily identified in the HCO^+ spectrum, which shows little emission (see Fig. 2). In addition to the three strong components at V_{LSR}=550, 544 and 539 km s^{-1}, several other features are apparent, especially at red-shifted velocities. The HCO^+ optical depths cover the full observable range from 0.2 to $\geq$2. Weaker components with $\tau \approx$0.1 may be present at the 2σ level on both the red and blue sides of the 550 km s^{-1} feature.

4.2. ^{12}CO, ^{13}CO and $C^{18}O$ absorption lines

The three central absorption components are clearly visible in the high-resolution ^{12}CO 1–0, 2–1 and 3–2 spectra presented in Fig. 2, and have similar appearances in the three transitions. The 550 km s^{-1} component is broad ($\Delta V \approx$5 km s^{-1}) and heavily saturated in all three transitions, whereas the 544 km s^{-1} component is very narrow, $\Delta V \approx$1.5 km s^{-1}; at high resolution, it is nearly as saturated as the 550 km s^{-1} component. The 539 km s^{-1} component is again wider with $\Delta V \approx$4 km s^{-1}. It has an asymmetric profile, suggesting that it is actually a blend of several narrow components. There are hints of additional CO absorption components at the velocities of the weaker HCO^+ components listed in Table 1. The errors in derived CO optical depths result mostly from uncertainties in the placement of the continuum.

Very few features are visible in the ^{13}CO spectrum (see Fig. 2). The optical depth of the 550 km s^{-1} component is 0.6, compared with $\tau \approx$0.7 found by Eckart et al. (1990). A

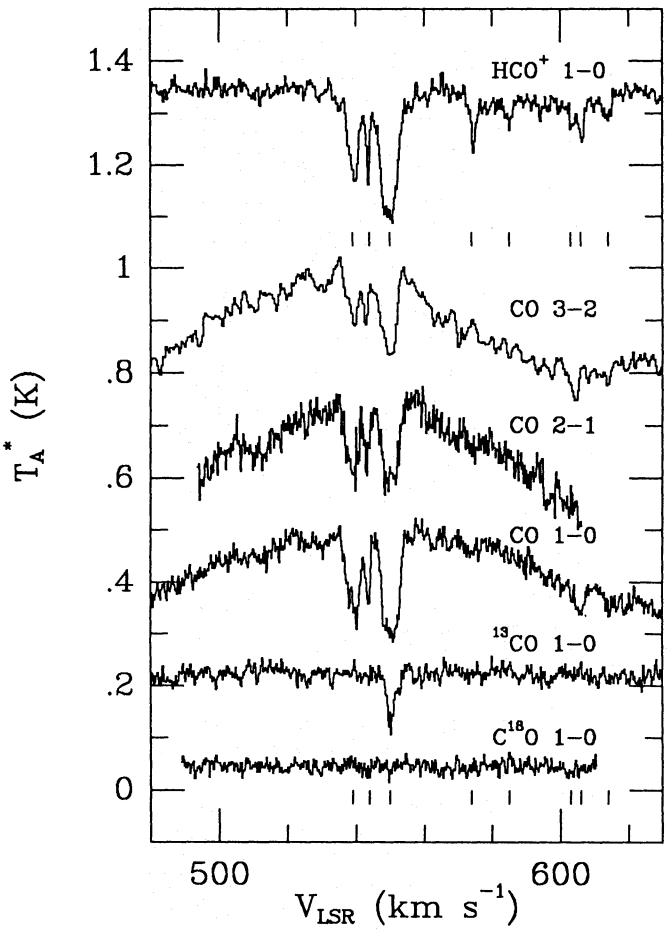

Fig. 2. High–resolution spectra of HCO^+ 1–0, ^{12}CO 3–2, 2–1 and 1–0, ^{13}CO 1–0 and $C^{18}O$ 1–0 toward the nucleus of Centaurus A. The spectra have been shifted in T_A^* by +1.05, +0.4, +0.25, 0.0, -0.05 K and -0.20 K, and have velocity resolutions of 0.29, 0.9, 0.23, 0.23, 0.23 and 0.23 km s^{-1}, respectively. Note the numerous absorption components in the HCO^+ spectrum at red–shifted velocities.

shoulder with $\tau \approx 0.2$ appears to be present on the red wing, suggesting that the 550 km s^{-1} component is also a blend of several narrower features. No ^{13}CO was detected at 539 km s^{-1}; the narrow 544 km s^{-1} component may be present with $\tau \approx 0.1$. The $C^{18}O$ spectrum shows a 2σ feature with $\tau \approx 0.15$ at 550 km s^{-1}.

5. Analysis

5.1. Method

The interpretation of millimetre absorption line data requires special attention, since observationally only optical depths can be determined. Statistical equilibrium calculations were performed for the 10 lowest levels of the CO molecule, and included the processes of collisional excitation and de–excitation, spontaneous emission, and stimulated absorption and emission in a background radiation field. Initially, this was taken to be the T_{bg}=2.7 K cosmic background radiation field. The radiative transfer was treated in terms of a mean escape probability. The physical parameters entering the calculations are the kinetic temperature T, the density of collision partners $n(H_2)$, and the column density divided by the line width, $N/\Delta V$. Each absorption feature was assumed to represent a single cloud, and the observed ΔV for unsaturated lines was adopted in the calculations. More details of the method will be presented in a future paper describing the excitation of a larger number of molecules (van Dishoeck et al., in preparation).

The analysis for CO is less straight–forward than for other molecules, owing to a peculiar effect in the CO excitation. As pointed out previously by Goldsmith (1972) and Koppen and Kegel (1980), population inversion occurs for the lowest levels at $T \gtrsim 30$ K and $n \approx 5000$ cm^{-3}. This does not lead to noticeable effects in emission spectra, but it results in CO 1–0 absorption optical depths close to zero for column densities less than 5×10^{16} cm^{-2} at these temperatures and densities. Thus, such warm and moderately dense components will not show CO or ^{13}CO 1–0 absorption, but they should be visible in the higher transitions.

5.2. The 550 km s^{-1} component

The CO column density in the strongest component at 550 km s^{-1} must be very large, for several reasons. First, the estimated visual extinction to the nucleus is 25±5 mag (Paper I), leading to $N(H_2)=(2\pm1)\times10^{22}$ cm^{-2}. If most of this extinction corresponds to the 550 km s^{-1} component, this would lead to $N(^{12}CO) \approx (2\pm1)\times10^{18}$ cm^{-2} for $CO/H_2 \approx 10^{-4}$. Second, the estimated ^{13}CO column density is $5\times10^{15}-5\times10^{16}$ cm^{-2} for a wide range of physical conditions. Assuming $^{12}CO/^{13}CO \approx 50$, $N(^{12}CO) \approx (0.3-3)\times10^{18}$ cm^{-2}. Finally, the possible $C^{18}O$ feature implies $N(C^{18}O) \approx 1\times10^{15} - 1\times10^{16}$ cm^{-2}, leading to a similar ^{12}CO value if $^{12}CO/C^{18}O$=500. We adopt $N(^{12}CO)=(1^{+1}_{-0.5})\times10^{18}$ cm^{-2}. For such large column densities, the computed optical depths in the 1–0, 2–1 and 3–2 ^{12}CO lines range from at least 3 to more than 100 for T=10–50 K and $n(H_2)=3\times10^2$–10^5 cm^{-3}. Such large optical depths are consistent with the observations, which show lines that are broadened by saturation, but unfortunately they do not constrain the physical conditions any further. In addition, the interpretation is complicated by the strong possibility that this component is actually a blend of several features, each representing a separate cloud at varying distance to the nucleus. More information may be obtained from ratios of the less saturated ^{13}CO lines. If we take the measured ratio $\tau(^{13}CO$ 2–1$)/\tau(^{13}CO$ 1–0$) \approx 0.6$–1 by Eckart et al. (1990) at face value, low temperatures $T \lesssim 20$ K *and* low densities $n \lesssim 1000$ cm^{-3} are found. Such low densities are inconsistent with the observation of other molecules in the 550 km s^{-1} component, and would require a large density gradient along the line of sight, with the CO molecules sampling the less dense regions. Alternatively, the ^{13}CO 2–1 optical depth may well have been underestimated: a higher ^{13}CO 2–1/1–0 optical depth ratio would allow higher densities or temperatures. The conclusions for CO are not significantly modified if the continuum radiation field by the nucleus is taken into account in the excitation calculations, provided that the CO molecules are at least 100 pc from the nucleus.

On the basis of the CO observations alone, it is difficult to determine temperature and density separately. Independent constraints can be obtained from the excitation of other molecules and from their chemistry, in particular from the

Table 1. Measured optical depths for absorption components in Centaurus A

Molecule	V_{LSR} (km s^{-1})							
	539	544	550	574	585	603	606	614
^{12}CO 1–0	$2.1^{+0.5}_{-0.4}$	1.5±0.4	≥3	0.15±0.08	≤0.15	0.25±0.09	0.31±0.05	0.23±0.09
^{12}CO 2–1	$1.8^{+0.8}_{-0.5}$	$1.9^{+0.8}_{-0.5}$	≥3	0.4±0.2	≤0.15	...	...	...
^{12}CO 3–2	$1.8^{+1.0}_{-0.5}$	$1.8^{+1.0}_{-0.5}$	≥3	≤0.3	≤0.3	≤0.3	0.4±0.2	≤0.3
^{13}CO 1–0	≤0.08	0.10±0.05	0.60±0.10	≤0.08	≤0.08	≤0.08	≤0.08	≤0.08
C^{18}O 1–0	≤0.1	≤0.12	0.14±0.07	≤0.1	≤0.1	≤0.1	≤0.1	≤0.1

HNC/HCN ratio. This ratio is near unity in cold clouds such as TMC–1, but only 0.1 in warm clouds such as Orion (Goldsmith et al. 1986). The observed ratio in the 550 km s^{-1} component is about 0.3 (van Dishoeck et al., in preparation), strongly suggesting a temperature around 30 K. This temperature agrees well with that inferred from the CO emission lines.

5.3. Other components

As a consequence of the peculiar CO excitation, the limit $\tau(^{13}\mathrm{CO})\leq 0.1$ for the 539 and 544 km s^{-1} components leads to rather weak limits on column density, $N(^{13}\mathrm{CO})\lesssim 10^{16}$ cm^{-2}, suggesting $N(^{12}\mathrm{CO})\lesssim 5\times 10^{17}$ cm^{-2}. If CO/H$_2\approx 10^{-4}$, this would imply $N(\mathrm{H_2})\lesssim 5\times 10^{21}$ cm^{-2}, corresponding to $A_V\lesssim 6$ mag, which is about the typical extinction caused by the dust lane. Such CO column densities are also close to the beam–averaged value derived from the CO emission in the dust lane. Thus, either of the two components, or both, could be due to clouds in the dust lane of Centaurus A at considerable distance from the nucleus. The measured ^{12}CO 3–2 optical depths for these two features are comparable to those for the 1–0 and 2–1 lines, excluding low temperature ($T\approx 10$ K), low density ($n\lesssim 1000$ cm^{-3}) solutions.

Similar excitation arguments apply to the weaker components at $V_{LSR}>550$ km s^{-1}. Wherever the CO 3–2 absorption is at least as pronounced as the 1–0 and 2–1 absorption, a low temperature, low density solution is excluded. A particularly interesting feature is provided by the absorption around V_{LSR}=606 km s^{-1}, which is quite prominent in the CO 3–2 and HCO$^+$ spectra. This appears to be a warm ($T\gtrsim 30$ K) and dense ($n\gtrsim 10^4$ cm^{-3}) molecular clump falling into the nucleus. In addition, strong H I absorption occurs at nearby velocities (van der Hulst et al. 1983). There is a striking difference in HCO$^+$/CO optical depth ratios between the various components: the red–shifted molecular features are more abundant in this ion than the 550 km s^{-1} feature or the 539 and 544 km s^{-1} components, indicating either enhanced cosmic ray ionization rates or shock–induced processes in these clouds. Such processes could also explain the large H I optical depths at red–shifted velocities.

6. Conclusion

The CO 2–1 and 3–2 emission profiles confirm the presence of the circumnuclear disk which we postulated on the basis of strong molecular absorption lines and the infrared continuum. The mean CO excitation temperature in the circumnuclear disk is about 25 K. Weaker absorption features are found at red–shifted velocities throughout the HCO$^+$ and CO spectra. These components appear to have physical and chemical characteristics that separate them from the molecular clouds in the main part of the disk. Further study of them is in progress.

Acknowledgements. The authors thank A. Quillen for assistance with the CO 3–2 observations.

References

Bell, M.B., and Seaquist, E.R. 1988, *Ap. J.*, **329**, L17.
Eckart, A., Cameron, M., Genzel, R., Jackson, J.M., Rothermel, H., Stutzki, J., Rydbeck, G., and Wiklind, T. 1990, *Ap. J.*, **365**, 522.
Ellison, B.N., Schaffer, P.L., Schaal, W., Vail, D., and Miller, R.E. 1989, *Int. J. of Infrared and mm Waves*, **10**, 937.
Gardner, F.F. and Whiteoak, J.B. 1976*a*, *Proc. ASA.*, **3**, 63.
Gardner, F.F. and Whiteoak, J.B. 1976*b*, *M.N.R.A.S.*, **175** 9P.
Goldsmith, P.F. 1972, *Ap. J.*, **176**, 597.
Goldsmith, P.F., Irvine, W.M., Hjalmarson, Å, and Elldér, J. 1986, *Ap. J.*, **310**, 383.
Israel, F.P., van Dishoeck, E.F., Baas, F., Koornneef, J., Black, J.H., and de Graauw, T. 1990, *Astr. Ap.*, **227**, 342.
Koppen, J., and Kegel, W.H. 1980, *Astr. Ap. Suppl.*, **42**, 59.
Phillips, T.G., Ellison, B.N., Keene, J.B., Leighton, R.B., Howard, R.J., Masson, C.R., Sanders, D.B., Veidt, B., and Young, K. 1987, *Ap. J.*, **322**, L73.
Phillips, T.G., Sanders, D.B., and Sargent, A.I. 1990, in *Submillimetre Astronomy*, eds. G.D. Watt and A.S. Webster (Kluwer, Dordrecht), p. 223.
Quillen, A.C., de Zeeuw, P.T., Phinney, E.S., and Phillips, T.G. 1991, *Ap. J.*, submitted.
Seaquist, E.R., and Bell, M.B. 1986, *Ap. J.*, **303**, L67.
Seaquist, E.R., and Bell, M.B. 1990, *Ap. J.*, **364**, 94.
Stutzki, J. 1990, *Protostar*, JCMT Newsletter #9, p. 10.
Van der Hulst, J.M., Golisch, W.F., and Haschick, A.D. 1983, *Ap. J.*, **264**, L37.
Van Gorkom, J.H. 1987, in *Structure and Dynamics of Elliptical Galaxies*, ed. T. de Zeeuw, IAU Symposium 127 (Reidel, Dordrecht), p. 421.